Catalysis Science & Technology

PAPER

View Article Online
View Journal | View Issue

Cite this: *Catal. Sci. Technol.*, 2014, 4, 1989

'From the mole to the molecule': ruthenium catalyzed nitroarene reduction studied with 'bench', high-throughput and single molecule fluorescence techniques†

Adela I. Carrillo,[a] Kevin G. Stamplecoskie,[a] M. Luisa Marin*[ab] and Juan C. Scaiano*[a]

Received 8th January 2014,
Accepted 9th March 2014

DOI: 10.1039/c4cy00018h

www.rsc.org/catalysis

Single molecule fluorescence microscopy techniques are used to complement conventional catalysis and high-throughput experiments in order to gain a complete picture of a model reaction. In these experiments a model nitroarene is reduced to an amine where, upon reduction, a red shift in absorption/emission, as well as an increase in emission, is observed. The reaction is studied under bulk reaction conditions by NMR spectroscopy and the fluorescence activation makes it possible to also study this reaction at the single molecule level. Fluorescence correlation spectroscopy is a valuable technique in supporting the proposed reaction mechanism and understanding the nature and duration of molecular 'visits' to catalytic sites, where both the starting material, nitroarene, and the amine product have an affinity for the catalyst.

Introduction

The last decade has seen a dramatic increase in the number and quality of tools available for studying catalytic processes. Thus, the conventional organic chemistry or "bench" approach can be combined with high throughput (HT) techniques that enable a combinatorial approach to optimize catalysts and reaction conditions.[1] Moreover, single molecule techniques make it possible to visualize how a single molecule arrives at a catalytic site and departs after catalytic conversion; a few examples of this type have been reported, normally using fluorescence changes as the reaction reporter.[2,3]

Single molecule, high throughput and bench studies have not been the subject of a single reaction study; yet, this approach that we describe as "from the mole to the molecule" is feasible today and should provide a unique, intimate understanding of reaction mechanisms; in the future such a combination may become a powerful tool for catalyst design and optimization.

In this study we utilize two new ruthenium supramolecular catalysts based on mesoporous silica[4] to examine the reduction of nitro aromatics by hydrazine in what we believe is the first report that combines powerful HT laboratory tools and single molecule fluorescence techniques to take us from the relatively large scale to the single molecule examination of the catalytic reduction of nitroarenes.

Our catalysts, Ru@SBA and Ru@MCM, containing ruthenium on mesoporous MCM-41 or SBA-15 according to TEM images (see Fig. S1 and S2 in the ESI†), have not been tested before in reductive processes, although they have been proven to be valuable in oxidative reactions leading to Wittig chemistry of alcohol precursors.[4] Other ruthenium-based mesoporous catalysts have been used in alkene reductions.[5] We have examined simple nitroarenes using HT tools as a methodology to identify the best reaction conditions. Selected reactions were also examined at a larger "bench" level to ensure that the conditions selected worked well under classical organic chemistry conditions. Having achieved this, a fluorogenic nitroaromatic compound bearing the nitronaphthalimide functionality was tested at the bench level and selected for single molecule studies (Scheme 1).

In the reaction in Scheme 1, reduction leads to an aminonaphthalimide which fluoresces strongly at around 540 nm, a convenient spectral region for single molecule studies. Beyond visualization of the reaction, this work combined with fluorescence correlation spectroscopy (FCS) reveals that molecules generated at the catalytic site spend more time at their nascent place than at randomly selected locations in solution.

[a] *Department of Chemistry and Centre for Catalysis Research and Innovation, University of Ottawa, 10 Marie Curie, Ottawa, Ontario K1N 6N5, Canada. E-mail: scaiano@photo.chem.uottawa.ca*
[b] *Instituto Universitario Mixto de Tecnología Química (UPV-CSIC), Universitat Politècnica de València, Avenida de los Naranjos s/n, 46022 Valencia, Spain. E-mail: marmarin@qim.upv.es*

† Electronic supplementary information (ESI) available: High-throughput experimental techniques, 1H NMR spectra of **NN-1** and **AN-2** used to determine conversions as well as single molecule fluorescence data for **NN-1** and two TIRF videos illustrating the reaction as it proceeds. See DOI: 10.1039/c4cy00018h

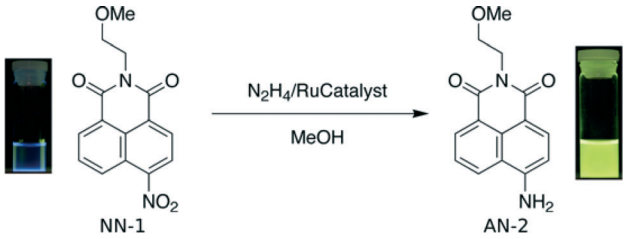

Scheme 1 Reductive conversion of **NN-1** to **AN-2** yields a strongly fluorescent product that is used as a reporter for fluorescence microscopy.

Thus, our work on two new catalysts brings us from the bench, or the 'mole' scale, to the molecule. We can envision a future in which single molecule and computational work will allow us to follow the reverse path, from the molecule to the mole, and scale-up to the industrial level with catalysts truly designed on the basis of an intimate understanding of how molecules achieve the desired transformation efficiently, rapidly and with high selectivity.

Ruthenium has received a lot of attention as a remarkably active catalyst in both homogeneous[6,7] and heterogeneous catalysis.[8] Ruthenium complexes have been used in metathesis as important catalysts that are both active and selective.[7,9] Recently Ru nanoparticles (RuNP) have been found to be active catalysts for hydrogenation[8,10] including asymmetric catalysis.[11]

If there is a drawback for using Ru as a catalyst, it is the high cost of the metal; Ru is considered a precious metal and is thus quite expensive. Therefore, to make Ru a viable catalyst it must be reusable, something that is easier to achieve with heterogeneous catalysts. One of the common questions in heterogeneous catalysis is whether the reaction is happening on the surface of the catalyst or as a homogeneous process in solution as a result of catalyst leaching from the particle surface.[12] One can adjust reaction parameters to gain some insight into the mechanism of the reaction, which is done here as well, but having a direct measure of the retention of reagents and products at the catalytic site is very valuable information in catalysis. Here we use a model reaction, such as shown in Scheme 1, to examine the catalytic activity of Ru nanoparticles (RuNP) supported on SBA. Using a combination of normal optical microscopy, total internal reflectance fluorescence (TIRF) microscopy and fluorescence lifetime imaging microscopy (FLIM) we are able to image both the catalyst and reaction species and in doing so better elucidate whether or not the reaction is happening on the surface of the catalyst.

Materials and methods

Materials

Tetraethyl orthosilicate (TEOS, 98%) was used as the silica source and cetyltrimethylammonium bromide (C_{16}TAB, 96%) or pluronic (P123) as the structure-directing agent. The aqueous ammonia solution (NH_4OH, 30%) and hydrochloric acid needed for the preparation of the mesoporous MCM-41 and SBA-15, respectively, and aminopropyltriethoxysilane (APTES) were also used in the synthetic protocol to obtain the final mesoporous material. $RuCl_3{\cdot}xH_2O$ was used as the ruthenium source; nitrobenzene, hydrazine monohydrate, other nitroaromatics and solvents were purchased from Aldrich and used as received without further purification. 1,3-Dimethoxybenzene and 1,3,5-trimethoxybenzene were from Alfa-Aesar. Nitronaphthalimide-1 (**NN-1**) was prepared according to a procedure described elsewhere.[13]

Catalyst preparation

The synthesis of MCM-41 or SBA-15 supported RuNPs was reported elsewhere.[4] Briefly, anhydrous toluene (50 mL) was added to dehydrated (473 K for 2 h) MCM-41 or SBA-15 (1.5 g) and this mixture was stirred for 1 h in order to obtain a homogeneous dispersion; then, APTES (0.5 mL) was added and refluxed overnight. The white solids obtained (silica–APTES) were filtered, washed with fresh toluene and acetone and air-dried. Then, ruthenium chloride ($RuCl_3{\cdot}xH_2O$, 9 mg) was added to an aqueous dispersion (110 mL) of the corresponding silica–APTES (1.5 g) and the resulting mixture was stirred for 1 h at room temperature. The grey solids obtained were filtered off and washed (H_2O) to remove the unreacted salt. The air-dried newly synthesized SRuNPs (2.5 wt% Ru, determined by ICP) were denoted as Ru@MCM or Ru@SBA.

Catalytic tests

High throughput combinatorial catalysis screening. The reactions were tested in plates containing 96 glass shell vials (8 × 40 mm), each with a π-arylene-coated tumble stir bar (ESI,† Fig. S1). The appropriate amount of the catalyst (10–25 mg) was manually weighed into each vial (accuracy of ±0.3 mg). Plates for reactions were prepared using a Symyx/Freeslate (Santa Clara, CA) first-generation core module, equipped with a Julabo LH45 temperature control unit. Nitrobenzene solutions in ethanol (0.6–1 M) were freshly prepared in 20 mL vials that were also loaded into the sample processor. The robot was programmed to dispense the appropriate substrate solution into each vial (ESI,† Fig. S2). Next, the plate was cooled down to 15 °C before the solution of hydrazine (6 M) was dispensed in order to avoid gas evolution. The appropriate amount of solvent (ethanol 99%) was programmed to be added to each vial to ensure an equal final volume of 0.5 mL. Finally, the internal standard (1,3,5-trimethoxybenzene) was added to every vial (0.030 mL, 0.5 M). Once every substrate solution was dispensed, the plate was sealed under air with a top metal plate consisting of a Teflon sheet and an aluminium cover, cushioned by two viton gaskets/sheets. Plates were stirred and heated on a VP Scientific VP710E-2/VP743A-1R microplate tumble stirrer. After that, the complete plate was centrifuged for 15 min in a Genevac EZ-2 Plus unit, and then aliquots were transferred to a new plate using the Symyx/Freeslate core module, diluted with ethyl acetate and loaded into the GC autosampler for analysis. Reactions were analyzed by a gas chromatograph (Agilent Technologies 6850 GC) equipped with a CTC GC-PAL autosampler and with a HP-1 column (30 m × 0.32 mm × 0.25 μm). The inlet/detector temperature was set at

250 °C and the initial oven temperature of 55 °C was held for 0.5 min followed by a ramp of 35 °C min^{-1} up to 120 °C held for 0.5 min and then a second ramp of 45 °C min^{-1} up to 260 °C held for 0.45 min (total runtime of 6 minutes). Retention times were confirmed by comparison with authentic materials when available or by injecting them into a GC-MS and comparing the retention times to those in the internal library. Yields of the reactions were determined from both consumption of the starting material and formation of the product. Peak areas were referenced against the internal standard, interpolating from previously made 7-points calibration curves. Agreement between replicate runs was within ±3%.

Optimized reduction conditions. In a typical run, to an ice-cooled mixture of 25 mg of Ru@SBA (4% mol) and 0.15 mmol of the nitroaromatic compound in 0.345 mL of EtOH, 0.125 mL of $NH_2NH_2{\cdot}H_2O$ 6 M (6 eq.) and 0.030 mL of the internal standard (1,3,5-trimethoxybenzene in the case of nitrobenzene or 1,3-dimethoxybenzene for the other nitro derivatives) (0.5 M) were added. The mixture was stirred under air at 80 °C for 21 h. Then it was centrifuged, and aliquots (0.020 mL of the reaction mixture were diluted up to 1 mL with AcOEt) were analyzed by GC or ^{1}H NMR.

Catalyst reusability. To check the reusability of the hybrid materials, they were washed three times with ethyl acetate by consecutive stirring and centrifuging steps. GC analysis of the last aliquot corroborated the absence of reaction products.

Microscopy measurements

Samples for microscopy were prepared by adding <1 mg of the prepared catalyst (Ru@SBA) into reaction wells with a cover slip bottom for imaging. 0.4 mL of methanol was added to the catalyst followed by 0.1 mL of a solution of the starting material (**NN-1**, 9.2 mM) and 0.010 mL of hydrazine (1.1×10^{-3} M). All measurements for single molecule catalysis were performed at room temperature; note that the reaction can be catalyzed even under these very mild conditions. The catalyst with methanol alone was imaged with white light as well as by fluorescence imaging that showed a contrast due to low intensity fluorescence and scattering of the catalyst. After addition of the starting material (**NN-1**), excitation at 375 nm was used to image the starting material and to obtain FCS curves of **NN-1** while focused on the catalyst or freely diffusing in solution. After addition of hydrazine, the product (**AN-2**) was excited selectively with 440 nm light to image **AN-2** in areas at the catalyst and diffused in solution. When excited by 440 nm (FLIM) or 480 nm (TIRF) light, the images were noticeably brighter as the reaction proceeded, as expected with the absorbance increase at longer wavelengths with formation of the product (see Fig. 4, *vide infra*).

Fluorescence activation reaction and controls

Benchtop control reactions were set up as follows: to a mixture of 10 mg of Ru@SBA (7.2% mol) and 10 mg (0.033 mmol) of **NN-1** in 1 mL of ethanol, 0.036 mL of $NH_2NH_2{\cdot}H_2O$ 6 M (6.5 eq.) were added. The mixture was stirred under air or H_2 atmosphere at 80 °C for 21 h in darkness. Then it was centrifuged, filtered off, concentrated and analyzed by GC and ^{1}H NMR.

UV spectroscopy and fluorescence

UV-vis spectra were recorded using a Cary UV-50 spectrophotometer. Steady state fluorescence spectra were recorded using a Photon Technologies International (PTI) fluorometer equipped with a Xe lamp for excitation, monochromators for both the excitation and emission and a PMT detector for detecting the fluorescence signal. Felix software was used to record and analyze fluorescence spectra.

Advanced microscopy

TIRF imaging. Fluorescence imaging was performed using an Olympus FV1000 TIRF (total internal reflection fluorescence) instrument (Olympus, Japan). The instrument is equipped with a 488 nm CW laser. The laser beam was collimated and focused through a fiber-coupling unit. A beam splitter cube was used with a dichroic mirror at 488 nm for the excitation, an excitation filter centred at 482 nm (18 nm bandpass) and an emission filter centred at 525 nm (45 nm bandpass). An oil immersion TIR (total internal reflection) objective (100×, NA1.45, Olympus, PLAPO) was used to focus both the excitation and emission, and the TIR images were recorded using a Rolera-MGi PLUS, a high-speed, extremely sensitive Digital EMCCD camera. Several frame TIRF images are presented in the ESI,† where the brightest/flashing spots correspond to the region in the catalyst where the amine product is generated and has an affinity for the solid. The same camera also collected white light images but using white light excitation from an Olympus TH4-100 powered 100 W halogen lamp.

FLIM and FCS. Fluorescence lifetimes, lifetime images and fluorescence correlation spectroscopy (FCS) curves were recorded using a Fluorescent Lifetime Imaging System (FLIM, PicoQuant).[3] The instrument is equipped with four picosecond pulse diode lasers including the 375 nm and 440 nm lasers used to excite the starting material and the product from Scheme 1, respectively. The laser beam was collimated and focused through a fiber-coupling unit. The same microscope and oil immersion TIR objective as that for TIRF measurements was used for the FLIM studies. Appropriate long pass filters were used to eliminate the excitation from the final FLIM images (400 LP for 375 nm excitation and 450 LP for 440 nm excitation).

FCS measurements were performed by focusing the excitation on regions that contained catalysts as identified by white light, TIRF and FLIM images, and were compared to FCS curves of regions that contained no catalyst (freely diffusing molecules in solution).

Results

Catalytic activity: reduction of nitroarenes

Because of the large number of variables that need to be examined to optimize a green process, such as the temperature,

reaction time, percentage of the catalyst and support or H_2 source, a combinatorial catalysis screening approach seemed appropriate to optimize the reaction conditions.

Initial attempts used nitrobenzene and hydrazine monohydrate or ammonium formate as hydrogen sources, since the use of H_2 and eventually high pressures was ruled out in the development of a green and sustainable process. In the presence of ammonium formate no conversion was observed regardless of other experimental conditions. Efforts were then focused on the optimization of the support, mol percent of the catalyst, and equivalents of hydrazine. A high-throughput screening approach proved extremely valuable for this process. As shown in Fig. 1, the hybrid materials Ru@MCM and Ru@SBA at 1.6–4 mol% in the presence of 1–8 equivalents of hydrazine were tested. At the end of the reaction time, the plate was centrifuged, diluted and analyzed by GC. Yields were determined from both consumption of the starting material and formation of aniline. As shown in Fig. 1, at least 5 equivalents of hydrazine were needed to achieve quantitative conversion of nitrobenzene in the presence of at least 3.2 mol% of the catalyst. Higher yields were always obtained when Ru@SBA was employed compared to Ru@MCM at the same mol percent. Next, the effect of the reaction time (4 to 24 h) and temperature (40 to 80 °C) was examined. Complete conversion was achieved after a 21 h reaction time. Several by-products were observed from the GC-MS analysis when temperatures lower than 70 °C were used.[14] On the other hand, increasing the temperature up to 80 °C resulted just in the formation of the desired aniline. Overall the best conditions were found using 4 mol% of Ru@SBA in the presence of 5 equivalents of hydrazine monohydrate at 80 °C for 21 h under air.

Chemoselectivity of the reduction was also investigated (results are summarized on Table 1). Excellent selectivities were obtained for the reduction of the nitroarenes with substituents such as –OCH_3 and –CN (entries 2–3). However, the reduction of 3-nitrostyrene (entry 4) resulted in the formation of 3-aminostyrene together with 3-ethylaniline (1.6 : 1). The use of lower temperatures (60 °C) and lower equivalence of hydrazine monohydrate did not increase the selectivity towards the nitro group. The already optimized reduction conditions were then applied to the "more substituted" naphthalimide **NN-1** (entry 5).

Moreover, the reusability of the hybrid materials was tested in the reduction of nitrobenzene under the optimized reaction conditions. Results are summarized in Fig. 2. The two catalysts, Ru@MCM and Ru@SBA, exhibited high recyclability; in fact, interestingly, higher yields were obtained after the second reuse of Ru@MCM. This is commonly attributed to catalyst activation in other words, generation of reactive sites while under reaction conditions. Results obtained using Ru@HMS are also included for comparison.[4]

Table 1 Catalytic reduction of different nitroarenes[a]

#	Substrate and product	Yield (%)
1		>99
2	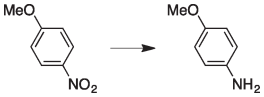	60
3	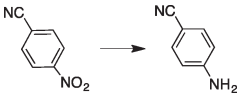	>99
4	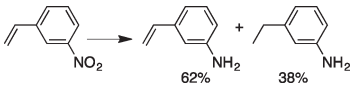	>99
5	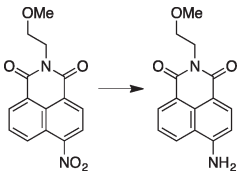	>99

[a] Nitroarene (0.15 mmol), Ru@SBA (4 mol%), hydrazine monohydrate (5 equivalents) in EtOH (99%) at 80 °C for 21 h under air.

Benchtop results: transition to single molecule studies

In order to use single molecule techniques and to move from the mole to the molecule, a material for reduction was required

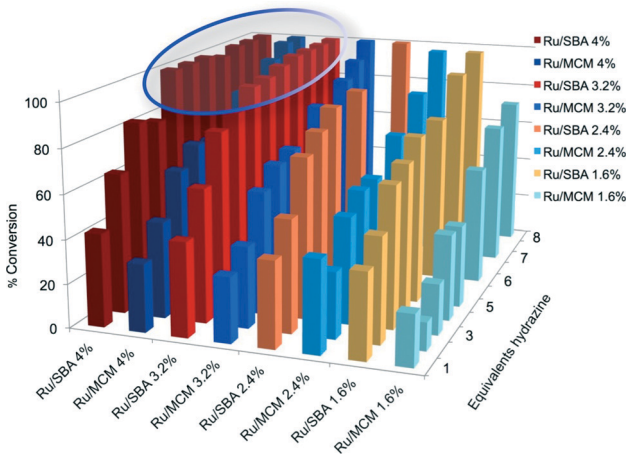

Fig. 1 Conversion of nitrobenzene as a function of the employed catalyst at various mol percentages and different equivalents of hydrazine monohydrate. The oval indicates the region of near-quantitative conversion as selected from the HT data.

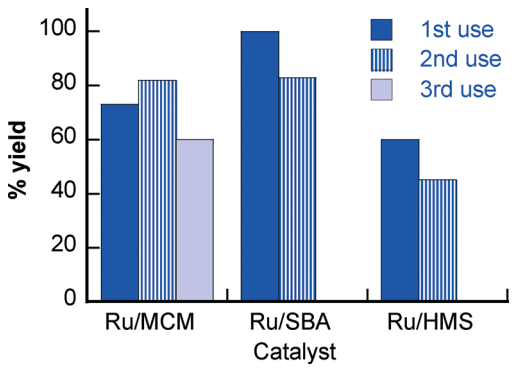

Fig. 2 Percentage of the reusability of the materials studied for the reduction of nitrobenzene under the optimized reaction conditions.

Table 2 Data from the benchtop reactions converting **NN-1** to **AN-2**. All reactions at 80 °C for 21 h

Entry	Conditions	Hydrazine monohydrate (equivalents)	Conversion[a] (% **AN-2**)
1[b]	Ru@SBA (7.2 mol%)	6.5	100
2	H_2 atmosphere	0	0
3	SBA (no RuNPs) H_2 atmosphere	0	0
4	Ru@SBA (7.2 mol%) H_2 atmosphere	0	≈6
5[b]	Ru@SBA (7.2 mol%)	0	0
6[b]	No catalyst or H_2	6.5	20[c]
7[b]	SBA	6.5	20[c]

[a] Determined by ^{1}H NMR. [b] Runs performed under air. [c] 100% conversion of starting material but only, 20% **AN-2**.

such that the reaction produces a fluorescent product different from the starting material. The nitro compound **NN-1** provided the requirements needed with a red shift and an increase in the emission quantum yield upon reduction to **AN-2**. The reaction was performed with the best catalyst (Ru@SBA) from the high-throughput experiments which required elevated temperatures (80 °C) to reach completion. For this reason, ethanol was used for benchtop reactions to reach higher temperatures, whereas methanol was sufficient as a solvent for the room temperature microscopy experiments.

The SBA supported RuNPs (Ru@SBA) catalyzed reduction of **NN-1** (Scheme 1) was first performed in bulk experiments (together with several control reactions – see Table 2) and analyzed by ^{1}H NMR and UV-vis absorbance and fluorescence spectroscopy. The absorbance and emission spectra of the reaction are shown in Fig. 3 (bottom), where a red-shift in both the absorbance and emission was observed. The product was identified by ^{1}H NMR as **AN-2** and it displays a 7× increase in maximum emission counts (see the ESI†).[13] The shift in absorbance and increase in the quantum yield of emission allowed for easy confirmation that the reaction had occurred.

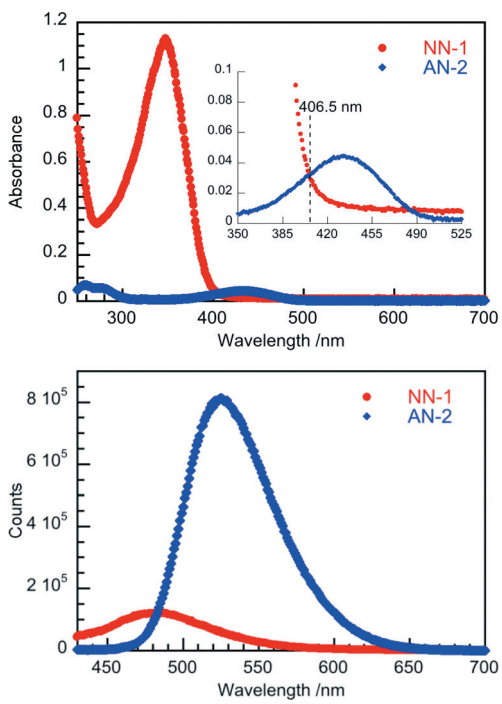

Fig. 3 Absorbance spectra of **NN-1** and **AN-2** (after reaction) (top) as well as (bottom) emission spectra of both compounds (with matched absorbance and excitation at 406.5 nm – see the ESI†).

^{1}H NMR spectroscopy was used to identify products and to quantify the conversion of the reaction shown in Scheme 1 (see the ESI†). The first entry in Table 2 shows that the reaction only goes to completion within 21 h when catalyzed by Ru@SBA. A minor conversion (6%) can be observed when the hydrazine reducing agent is replaced by a H_2 filled balloon (entry 4). While complete conversion of the starting material is observed without Ru@SBA in the same amount of time (entry 6) and no starting material remained unreacted, only 20% conversion to **AN-2** could be achieved.

Microscopy. The ^{1}H NMR product analysis shows that the Ru supported catalysts increase the reaction rate as well as the fact that addition of the less efficient H_2 gas instead of hydrazine as the reducing agent works most effectively with the Ru catalyst present. Both results suggest that the reaction occurs at the surface or, at the very least, is activated by the catalyst. In order to further establish if the reaction occurs on the catalyst, single molecule fluorescence is used to follow the variations in diffusion of the **NN-1** and **AN-2** (Scheme 1) in solution as compared with the catalyst. When a laser is focused on a spot, fluorescence correlation spectroscopy (FCS) can be used as a measure of the average time molecules spends within that focused spot. Therefore, comparing FCS plots when the laser is focused on the catalyst or if it is focused in solution (after some **AN-2** product has accumulated) gives different results if there are some binding affinities for the surface.[15] Using a 440 nm laser, the products of the reaction can be selectively excited (Fig. 3). In this way, the image in Fig. 4 was recorded, with the brightest spots in the FLIM images corresponding to the catalyst (confirmed by white light and TIRF images similar to those in the ESI† where the starting material image is shown). Representative FCS traces of the catalyst and solution spots are given in Fig. 4 as indicated.

A direct comparison of representative FCS curves of a catalyst spot and a solution spot is given in Fig. 5. The catalyst spots consistently show a longer τ, indicating that the products spend more time on the catalyst than freely diffusing through solution. Similar images and FCS traces were recorded for the starting material with 375 nm excitation

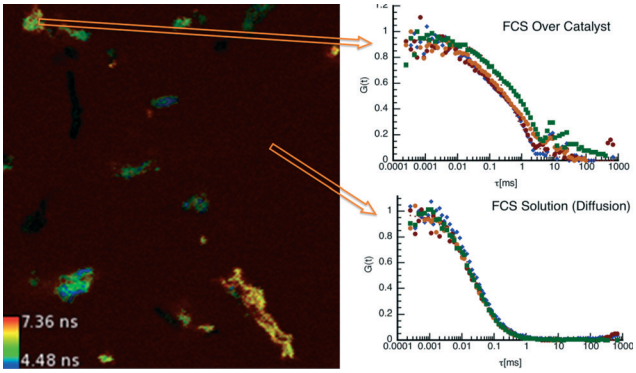

Fig. 4 FLIM image acquired with 440 nm laser excitation during reduction of **NN-1**, where the bright spots correspond to the catalyst (left). FCS curves when focused on the catalyst spots (top right) and solution spots (bottom right). Solution spots were measured after some accumulation of the product **AN-2**.

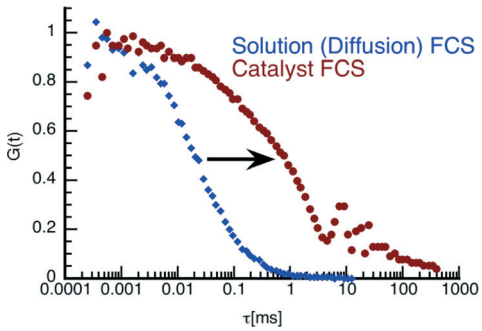

Fig. 5 Representative FCS curves with 440 nm excitation when excitation/image acquisition is focused on either a catalyst (red) or solution (blue) spot.

(see the ESI†). A similarly longer τ is observed for the starting material on the catalyst as compared to in solution, indicating some binding to the catalyst of the starting material as well. These results are consistent with the reaction being catalyzed at the surface through binding since both the reagents and products have an affinity for the surface. These experiments cannot distinguish between retention at the external or internal surface of a mesoporous material.

The curves in Fig. 5 suggest that the residence time of **AN-2** in the laser focal area increases from about 25 μs to about 1 ms where the latter corresponds to a nascent product at the catalytic site. The former (25 μs residence time) corresponds to **AN-2** in solution, added as a control and is not a reaction product.

Videos showing reaction triggered bursting are available as ESI.† They reveal multiple catalytic sites within a single particle and bursting spots at repeat locations; this is characteristic of reactions occurring at specific catalytic sites, presumed to be ruthenium-rich spots although diffraction limitations prevent us from visualizing these. Visual analysis of peaks and valleys in enlarged images such as those in Fig. 6 suggests that the 'hot' catalytic spots on SBA are located roughly 0.5 to 2 μm apart. The data were recorded at

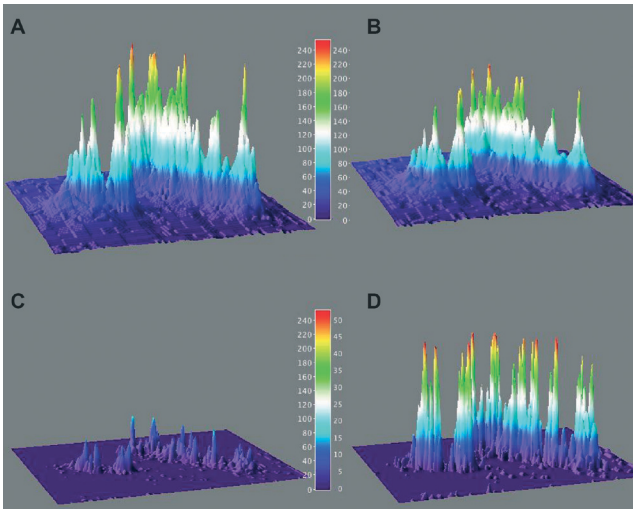

Fig. 6 3D plots of the accumulated emission intensity over a catalyst surface for 25 s (A) and for the following 25 s (B), a difference spectrum of (A) and (B) shown in (C) and a rescaled image of (C) at 5× the scale of (A), (B) and (C) shown in panel (D). The area displayed is 15.75 × 22.5 μm.

a rate of 10 frames per second for 50 seconds and are displayed in a cumulative way in Fig. 6, where panels A and B display the accumulated data for frames 1–250 (25 s) and 251–500 (next 25 s), respectively. While not identical, both panels show the same pattern and visually appear to have a similar intensity. The difference between panels A and B is shown in panel C at the same vertical scale as A and B and expanded 5× in panel D. Importantly, the peaks in panel D, while minute compared with A and B, are all positive revealing that the rate decreases slightly as the reaction progresses, not surprising as the reagents are being consumed.

Discussion

A common question for heterogeneous catalysis in liquid systems is whether or not the reaction is happening at the surface of the catalyst or in solution. In other words, do heterogeneous catalysts promote homogeneous catalysis through ion leaching mechanisms?[12]

Table 2 summarizes the results for the reaction in Scheme 1 (selected for single molecule work) as well as for control reactions. From the table of results, it is clear that the reaction is catalyzed by the RuNP supported on SBA as it is the only entry with complete conversion of **NN-1** to **AN-2**. Gas evolution is observed upon addition of hydrazine to solutions of the catalyst, presumably due to H_2 evolution. Therefore, it was thought to be possible that this reaction could occur by H_2 reaction with **NN-1** in solution and that the catalyst merely facilitates the oxidation of hydrazine to produce H_2. For this reason, the reaction was tested with saturated solutions of H_2 gas rather than hydrazine as the reducing agent (entries 2, 3 and 4 in Table 2). With the catalyst present and under a H_2 atmosphere, only 6% conversion was observed as compared with 100% conversion when hydrazine

was used. This indicates that the catalyst has a more important role than the mere release of H_2 from hydrazine to the reaction solution. In fact, this is consistent with the idea that hydrazine activation occurs at the catalyst surface.

Microscopy studies, and in particular FCS curves, can be used to examine the binding of both the starting material and products of the reaction with 375 nm and 440 nm excitation, respectively. The results indicate that both the starting material and products have an affinity for the catalyst, spending more time bound to the surface than diffused in solution. Since the FCS curves eventually drop to zero in all cases, this indicates that not only are they binding to the catalyst but the binding appears reversible, as expected for an efficient catalytic process. If the binding was irreversible, residual fluorescence would remain constant over time. From these results and the **NN-1** conversion studies, we propose a mechanism for this reaction that involves the RuNP activation of hydrazine as well as the surface catalyzed reduction of **NN-1** to **AN-2** (Scheme 2).

The microscopy studies reveal that catalysis consistently occurs over regions that are consistent with catalyst support seen in normal optical microscopy,[12,16] thus demonstrating that reaction occurs at the catalyst as opposed to in solution as the result of soluble catalyst leaching.[17] Further, comparison of sequential groups of frames shows that there is a slight decrease in the rate as the reaction proceeds (Fig. 6); beyond the obvious decrease due to the reagent's gradual depletion, there may be a small decrease of catalytic activity, as suggested also by the data in Fig. 2. Further, FCS studies reveal that once the reaction occurs, the product stays at the catalyst site for about 1 ms; clearly, strategies that reduce this unproductive product retention could enhance the overall catalytic efficiency. The mechanism proposed involves reduction by activated hydrogen generated on the catalyst surface; however, simply making H_2 available does not lead to comparable reduction levels.

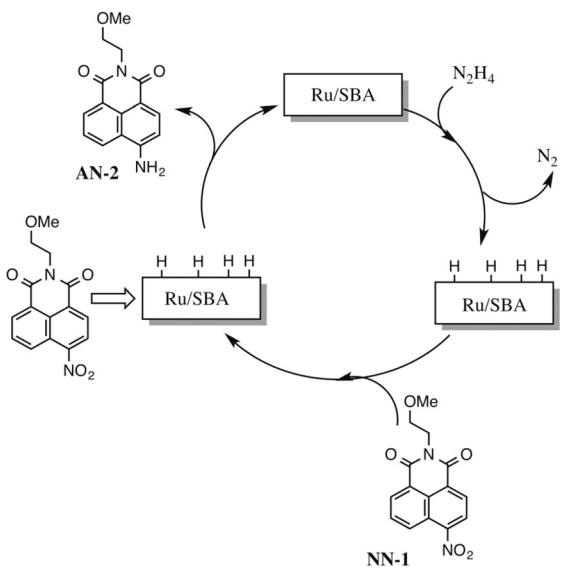

Scheme 2 Proposed mechanism for the Ru@SBA catalyzed reduction of nitro compounds to yield amines, illustrated for **NN-1**.

Conclusions

RuNPs highly dispersed in the channels of SBA have given excellent yields when catalyzing the reduction of nitroarenes under air at 80 °C using hydrazine monohydrate as the reducing agent. The experimental conditions were optimized based on a high-throughput screening analysis. From high throughput screening of reactions and benchtop reduction of **NN-1** to **AN-2** to single molecule microscopy experiments, we examine the reduction reaction 'from the mole to the molecule'. The rationale for this approach is to elucidate a complete picture of the mechanism of this reaction by performing single molecule spectroscopy on systems that can be tested on a large scale, where the catalyst and the catalytic conditions have been optimized.

In order to be able to use single molecule microscopy techniques, we used a model reaction with fluorescence activation to study the activity of SBA supported RuNPs as a catalyst for the reduction of nitro compounds to amines. The reduction results in a red-shift in absorption/emission as well as a fluorescence quantum yield increase. Single molecule fluorescence microscopy techniques results are consistent with the proposed reversible binding of the reaction species to the catalyst, the proposed mechanism of hydrazine activation as well as the reduction of the nitro compound on the catalyst surface. Overall, this example not only shows the selective activity of this RuNP catalyst towards reduction of nitro compounds to amines but also provides an example of how advanced microscopy techniques, in particular FCS and TIRF, can be advantageous in establishing catalytic mechanisms.

We anticipate that in the near future it may be possible that the use of the reverse approach "*from the molecule to the mole*" combined with recent advances in computational catalysis[18] will become a powerful tool in the design, optimization and scale-up of catalytic processes.

Acknowledgements

Thanks are due to the Natural Sciences and Engineering Council of Canada and the Canadian Foundation for Innovation for generous support. M.L. Marin thanks the Universitat Politécnica de Valencia (Programa de Apoyo a la Investigación y Desarrollo) for financial support. Technical support from Roxanne Clement at uOttawa's Centre for Catalysis Research and Innovation is gratefully acknowledged.

References

1 S. R. Stauffer and J. F. Hartwig, *J. Am. Chem. Soc.*, 2003, **125**, 6977; A. McNally, C. K. Prier and D. W. C. MacMillan, *Science*, 2011, **334**, 1114.

2 M. B. J. Roeffaers, G. DeCremer, J. Libeert, R. Ameloot, P. Dedecker, A.-J. Bons, M. Bçkins, J. A. Martens, B. F. Sels,

D. E. DeVos and J. Hofkens, *Angew. Chem., Int. Ed.*, 2009, **48**, 9285; M. B. J. Roeffaers, J. Hofkens, G. DeCremer, F. C. DeSchryver, P. A. Jacobs, D. E. DeVos and B. F. Sels, *Catal. Today*, 2007, **126**, 44; T. Tachikawa and T. Majima, *Langmuir*, 2012, **28**, 8933; X. Zhou, W. Xu, G. Liu, D. Panda and P. Chen, *J. Am. Chem. Soc.*, 2010, **132**, 138.

3 T.-L. Wee, L. C. Schmidt and J. C. Scaiano, *J. Phys. Chem. C*, 2012, **116**, 24373.

4 A. Carrillo, L. Schmidt, M. L. Marin and J. C. Scaiano, *Catal. Sci. Technol.*, 2014, **4**, 435.

5 C. del Pozo, A. Corma, M. Iglesias and F. Sanchez, *Green Chem.*, 2011, **13**, 2471; J. Hájek, N. Kumar, P. Mäki-Arvela, T. Salmi, D. Y. Murzin, I. Paseka, T. Heikkilä, E. Laine, P. Laukkanen and J. Väyrynen, *Appl. Catal., A*, 2003, **251**, 385.

6 C. K. Prier, D. A. Rankic and D. W. Macmillan, *Chem. Rev.*, 2013, **113**, 5322.

7 A. Szadkowska, C. Samojłowicz and K. Grela, *Pure Appl. Chem.*, 2011, **83**, 553.

8 P. Lara, K. Philippot and B. Chaudret, *ChemCatChem*, 2012, **5**, 28.

9 R. H. Grubbs, *Handbook of Metathesis*, Wiley-VCH, Weinheim, 2003.

10 S. Jansat, D. Picurelli, K. Pelzer, K. Philippot, M. Gómez, G. Muller, P. Lecante and B. Chaudret, *New J. Chem.*, 2006, **30**, 115.

11 G. Salas, P. Campbell, C. Santini, K. Philippot, M. Costa Gomes and A. Pádua, *Dalton Trans.*, 2012, **41**, 13919.

12 I. W. Davies, L. Matty, D. L. Hughes and P. J. Reider, *J. Am. Chem. Soc.*, 2001, **123**, 10139.

13 L. A. Montoya and M. D. Pluth, *Chem. Commun.*, 2012, **48**, 4767.

14 J. W. Larsen, M. Freund, K. Y. Kim, M. Sidovar and J. L. Stuart, *Carbon*, 2000, **38**, 655.

15 W. Al-Soufi, B. Reija, M. Novo, S. Felekyan, R. Kühnemuth and C. A. M. Seidel, *J. Am. Chem. Soc.*, 2005, **127**, 8775.

16 C. A. Witham, W. Huang, C.-K. Tsung, J. N. Kuhn, G. A. Somorjai and F. D. Toste, *Nat. Chem.*, 2010, **2**, 36.

17 Y. Nishina, J. Miyata, R. Kawai and K. Gotoh, *RSC Adv.*, 2012, **2**, 9380.

18 J. K. Norskov, T. Bligaard, J. Rossmeisl and C. H. Christensen, *Nat. Chem.*, 2009, **1**, 37.

